Title

Age-dependent Deformation of the Optic Nerve Head and Peripapillary Retina by Horizontal Duction.

Authors

Le, Alan
Chen, Jessica
Lesgart, Michael
et al.

Publication Date

2020

DOI

10.1016/j.ajo.2019.08.017

Peer reviewed

HHS Public Access

Author manuscript

Am J Ophthalmol. Author manuscript; available in PMC 2021 January 01.

Published in final edited form as:

Am J Ophthalmol. 2020 January ; 209: 107–116. doi:10.1016/j.ajo.2019.08.017.

Age-dependent Deformation of the Optic Nerve Head and Peripapillary Retina by Horizontal Duction

Alan Le[1,2,3], **Jessica Chen**[4], **Michael Lesgart**[5], **Bola A. Gawargious**[6], **Soh Youn Suh**[1,2], **Joseph L. Demer**[1,2,3,7,8]

[1]Department of Ophthalmology, University of California, Los Angeles.

[2]Stein Eye Institute, University of California, Los Angeles.

[3]Bioengineering Interdepartmental Programs, University of California, Los Angeles.

[4]Computational and Systems Biology Interdepartmental Program, University of California, Los Angeles.

[5]Department of Psychology, University of California, Los Angeles.

[6]Department of Integrative Biology and Physiology, University of California, Los Angeles.

[7]Department of Neurology, University of California, Los Angeles.

[8]David Geffen Medical School at University of California, Los Angeles.

Abstract

Purpose: We studied effects of age and horizontal duction on deformation of the optic nerve (ON) head and peripapillary retina as reflected by displacement of vascular landmarks to explore the influence of adduction tethering.

Design: Cross-sectional study.

Methods: *Setting:* University.

Study Population: Single eyes of 20 healthy young adults (average age 23.9±3.9 SD) years were compared to 20 older subjects (average age 61.4±9.3) years. Observational *Procedure:* The disc and peripapillary retina were imaged by scanning laser ophthalmoscopy in central gaze, and 35° abd- and adduction.

Main Outcome Measure: Deformations of the disc and adjacent PPR were measured by comparing positions of epipapillary and epiretinal blood vessels.

Results: Vessels within the ONH of younger subjects shifted temporally during adduction and nasally during abduction. Displacement of the nasal hemi-disc in adduction was greater at 38.5±1.7μm (SEM) than the temporal half at 4.1±2.1μm (P<0.001). Peripapillary retina within one

Address for Correspondence and Reprints: Joseph L. Demer, M.D., Ph.D., Stein Eye Institute 100 Stein Plaza, UCLA, Los Angeles, California, 90095-7002 U.S.A. Telephone: 310-825-5931. Facsimile: 310-206-7826, jld@jsei.ucla.edu.

radius of the disc margin underwent 7.6±1.6μm average temporal displacement in adduction in young subjects. In abduction, the young temporal hemi-disc shifted 4.4±0.6μm nasally without significant displacement in the nasal half. Older subjects' ONH showed less temporal shift and less displacement in the PPR within one disc radius ($P<0.0001$) in adduction; the nasal hemi-disc shifted 24.5±1.3μm compared with 4.4±2.1μm in the temporal half. There were no significant deformations of the disc during abduction by older subjects.

Conclusion: Large horizontal duction, particularly adduction, deforms the disc and peripapillary vasculature. This deformation, which is larger in younger than older subjects, may be due to ON tethering in adduction.

INTRODUCTION

When the human eye rotates into large angle adduction, magnetic resonance imaging (MRI) demonstrates that the optic nerve (ON) and the optic nerve dural sheath (ONS) straighten, become tethered, and exert traction on the posterior globe.[1,2] Resulting anteroposterior deformations of posterior ocular tissues during horizontal duction have been demonstrated by two-dimensional optical coherence tomography (OCT), including anteroposterior tilting of the ON head (ONH) and peripapillary Bruch's membrane.[2,3,4] The nasal side of the ONH moves anteriorly while the temporal side moves posteriorly.[2,5] The effect is greatly enhanced with adduction exceeding a threshold of about 26°. Saccades of 25–45° are comm on during everyday eye movement[6] and can rotate the eyes beyond this threshold. Gaze shifts with head rotation includes eye movements averaging ~30°.[78] In abduction, the ONH also exhibits see-saw motion directionally inverse to abduction.[3,9] While both abduction and adduction can deform the ONH, the effect is greater for adduction, presumably due to ON tethering. This is likely why our previous MRI study found no optic nerve tethering in exotropia, but higher occurrence in esotropia.[5]

Biomechanical studies of stress and strain in the posterior eye using finite element analysis have focused on the structural properties of the ONH, peripapillary sclera and lamina cribrosa to suggest possible mechanisms of glaucoma independent of intraocular pressure (IOP).[10–13] Elevated IOP can of course produce mechanical stress in the ONH,[10,14,15] yet IOP alone cannot alone explain glaucomatous optic neuropathy in many patients with normal or subnormal IOP that accounts for a majority of glaucoma cases in Asian populations.[16,17] It has been proposed that force concentration in peripapillary sclera due to eye movements may be an IOP-independent mechanism for ONH deformation leading to glaucomatous optic neuropathy,[18] since by this mechanism, strain is concentrated on the temporal side of the ONH where peripapillary atrophy most commonly occurs, as does the earliest damage in glaucoma.[19]

Although peripapillary mechanical deformation is greatly exaggerated in adduction where the ON becomes tethered, eye rotation also deforms this region during smaller ductions. In papilledema, Sibony showed distortion of the peripapillary basement membrane during horizontal duction even without ON tethering.[9] Wang *et al.* demonstrated by OCT in normal subjects that there are ONH strains during even moderate abduction and adduction.[20]

Previous OCT studies of horizontal duction examined anteroposterior shifts and tilts of the ONH, but did not investigate possible horizontal and vertical deformations. Examination of the ONH by OCT is often confounded by shadows cast by epipapillary blood vessels (BVs) obscuring much of the underlining tissue. We have explored an alternative approach of *en face* imaging that exploits these same BVs as fiducial landmarks to study local horizontal and vertical displacements in the ONH and surrounding retina produced by gaze changes. Local deformations of the ONH and retinal surface can be deduced from differential translational shifts in local features. In the current study, we tracked large BVs on the retinal and ONH surfaces as markers of local deformation of the underlying tissues. We investigated whether horizontal ductions differently displace BVs in subjects of different ages.

METHODS

Subjects

Twenty healthy young adult volunteers (11 males, 9 females) of mean age 23.9±3.9 (SD, range 19–32) years and 20 healthy older volunteers (7 males, 13 females) of mean age 61.4±9.3 (range 48–79) years were recruited by advertising and examined to verify absence of ocular disorders besides correctable refractive error. Subjects were provided written, informed consent prior to participation according to a protocol approved by the University of California, Los Angeles Institutional Review Board compliant with the Declaration of Helsinki. All subjects underwent comprehensive eye examinations to confirm normal corrected visual acuity, normal binocular alignment, and normal IOP (<21mmHg) without evidence of glaucomatous optic neuropathy. Only the right eye of each subject was analyzed. There were no high myopes or high hyperopes, defined as having more than 5 D spherical equivalent refractive error. Of the total 40 subjects studied, 26 had uncorrected visual acuity at least 20/20, and so represent emmetropes or low hyperopes.

Of the younger volunteers, 12 were Caucasian and 2 each of African American, East Asians, South Asians, and Middle Easterners. The older group included 12 Caucasians, 4 African American, 1 East Asian, and 3 Middle Eastern.

En face Infrared Imaging

The infrared scanning laser ophthalmoscope mode of a Heidelberg Spectralis scanner (Heidelberg Engineering, Heidelberg, Germany) was used to image the ONH and adjacent retina. A retinal nerve fiber layer (RNFL) circular scan was first performed to verify normal thickness. Each right eye was then imaged in central gaze, 35° abduction, and 35° adduction sequentially by rotati ng the imager camera to calibrated angles on its azimuth pivot, including central gaze and 35° ab- and adduction. The scanner rotated along with the eye thus maintaining a constant angle relative to the line of sight. The subject's head was stabilized to the scanner headrest using cushions and straps to prevent head rotation. To obtain images centered on the ONH, subjects fixated the scanner's internal target that, by manufacturer's design, is offset 12° nasally from straight-ahead; this offset was compensated by a custom goniometric scale to set desired ductions. During eccentric gaze imaging in some subjects, the camera was also translated towards the subject to obtain the desired gaze

angle to clear the nose and other facial features. This anteroposterior camera translation changed image magnification slightly but this was corrected during analysis. En face images were exported at 5.85μm/pixel.

Large BVs on the retinal and ON surface were used as fiducials to track local deformations of the underlying tissues to which they are attached. Figure 1 shows a major BV branch traced during central gaze (1A green) and adduction (1C red). Figure 1B superimpose the green and red paths, highlighting relative displacement between gazes. Dotted green and red paths in the figure are shown for representation of major BV displacement.

B-Scan OCT

Subjects were imaged using in the OCT mode with enhanced depth imaging of the ONH and peripapillary retina (PPR). The B-scans were assessed for vitreous attachment.

Image Analysis

Images were exported as tagged image file format (TIFF) files and processed using Adobe Photoshop (Adobe Systems, San Jose, CA, USA). In subjects who required translation of the OCT camera to focus the retina, magnifications of images obtained in ab- and adduction were isotropically scaled to match the size of the central gaze image. In all cases, the resulting three images for each eye were superimposed in a digital stack for analysis. Images obtained in ab- and adduction were rotated and translated to match the central gaze image using BVs remote from the ONH as anchor fiducials; this approach compensates for physiologic ocular torsion in eccentric gazes resulting from Listing's Law[21]. A circular grid (Fig. 2) with 5 concentric rings divided radially into 8 sectors was overlaid on the image stack. The center ring had diameter equal to the ONH, and each successive ring had an integer multiple of the center diameter, dividing the retina into concentric regions. Region 0 represented the ONH. Region 1 enclosed the area 1 disc radius beyond the ONH border. Region 2 extended an additional disc radius from Region 1, Region 3 the next disc radius, and Region 4 extended a further disc radius beyond Region 3 to a maximum of 4 disc radii from the ONH. Each of the five regions was divided into 8 equal sectors numbered clockwise from the top as shown in Fig. 2.

Whenever one or more BV intersections or branch points were present in each of the 40 zones, a marker was placed on each feature, thus demarcating fiducials that permitted robust tracking of underlying retinal displacements associated with changes in gaze direction. By alternating the opacity of images obtained in abduction and adduction superimposed on the central gaze image, displacements caused by the gaze change were tracked for each marker.

Each of the three image layers had associated marker fiducial layers that represented BV intersections or branch points in each sector containing such features (Fig. 3). *ImageJ64* (W. Rasband, National Institutes of Health, Bethesda, Maryland, USA; http://rsb.info.nih.gov/ij/, 1997–2018, in public domain) was used to compensate magnification variations, and to determine the location of each fiducial. Custom programs then calculated horizontal and vertical displacements of fiducials for each gaze position. Software written in the MATLAB (MathWorks, Inc, Natick, Massachusetts) software suite was used to plot heatmaps of the displacements.

Statistical Analysis

Using GraphPad Prism (GraphPad Software, San Diego, CA), horizontal and vertical displacements of fiducials from central to 35° ab- and adduction were compared using paired t-tests significant differences from zero and between age groups at the 95% confidence level. All measurements were repeated by a second analyst. Results by the two analysts did not differ significantly.

RESULTS

Horizontal Displacements

Adduction to 35° temporally shifted vessels intrins ic to the ONH in both young and elderly subjects, indicting displacement of the ONH itself. In young subjects (Fig. 4), all sections (1–8) overlying the ONH (Region 0) exhibited significant temporal displacement ($P<0.0001$) with the largest displacement in Section 2 (41.7±5.8μm SEM), which is the superonasal disc. The entire nasal half (Sections 1–4) of the ONH were displaced more on average than the temporal half (Sections 5–8) at 4.1±2.1μm ($P<0.001$). The PPR (Region 1) extending one disc radius from the ONH was significantly displaced temporally in all sections but Sections 6 and 7, averaging 7.6±1.6μm (Figs. 4 and 5). There was less displacement farther than one disc radius from the ON center; in Region 2, only Section 8 was significantly displaced in adduction. There were no significant horizontal displacements in the more distal Regions 3 and 4. Abduction shifted vessels in and near the ONH nasally, but less than in adduction; there were no displacements beyond the ON border (Regions 1–4) in abduction.

In older subjects (Figs. 6 and 7), 5 of the 8 sectors within the ONH exhibited significant temporal displacement in adduction but not in abduction. In adduction, the nasal half sections of the ONH shifted more on average at 24.5±1.3μm than the temporal half sections at 4.4±2.1μm ($P<0.001$). While there were no displacements in Regions 2 – 4, four sections adjacent to the ON (Region 1) significantly shifted temporally by an average 2.0±0.4μm during adduction. No significant displacements in abduction occurred anywhere in older subjects.

Vertical Displacements

Adduction to 35° caused much smaller vertical than horizontal displacements in both young and older subjects ($P<0.001$, Figs. 8 and 9). In younger subjects there were 4 zones exhibiting deformation: Region 0, Section 4, and Region 2 Sections 5 and 8 shifted superiorly, while Region 1, Section 1shifted inferiorly. Abduction produced small inferior shifts in the ONH and three zones of Region 1. The superior half of the ONH in older subjects (Fig. 9) shifted inferiorly in adduction, although only two zones exhibited small vertical displacement (<3.2μm) during abduction. All vertical displacements were smaller than horizontal displacements.

Effect of Posterior Vitreous Detachment (PVD)

Standard B-scan OCT was employed to examine the relationship of the vitreous body to ON and peripapillary displacements during horizontal duction. Of the 20 older subjects, 12 had complete PVD and 8 had partial PVD. Displacements during horizontal duction were similar

regardless of vitreous attachment. Vitreous detachment was not significantly associated with horizontal and vertical displacement in ab- or adduction (P> 0.6).

Vascular Pulsatility

Pulsating vessels on the ONH were observed in six of the younger subjects in *en face* imaging. Movement of superficial BV due to pulsatility was confined to the ONH surface, was only in the anteroposterior direction, and had very small magnitude (<10 μm). No significant horizontal and vertical fiducial shifts resulted from vascular pulsatility. No vascular pulsatility was observed in older subjects.

DISCUSSION

Deformation of the ONH has been linked to reduction in RNFL thickness and gradual visual loss in glaucoma.[22–26] While many studies focus on elevated IOP as a cause of short term ONH deformation, some recent studies have demonstrated that eye movements can also deform the ONH, and so may represent a pathological process when repeated many times during the very large number of everyday eye movements.[1] The current study provides further evidence that horizontal ductions not only deform the superficial ONH but also the surrounding PPR. Whereas prior OCT studies measured anteroposterior movement of Bruch's membrane[3] and ONH tilt angle[2], our current study quantified local horizontal and vertical translational shifts of large blood vessels embedded in the ONH and retinal surface. Extending previous OCT studies,[2,3] the current *en face* imaging shows that the nasal half of the ONH moves temporally in addition to what was already known to be anteriorly, during adduction, and conversely the nasal half of the ONH moves slightly nasally in addition to what was already known to be posteriorly during abduction. The nasal half of the ONH is thus compressed during adduction more than during abduction. Vertical deformations were minimal during horizontal ductions, in both younger and older subjects.

The blood vessels tracked in this study were embedded in or adherent to the ONH and PPR with which they are intimately associated. Movements of papillary and peripapillary retinal blood vessels indicate movements of these neural tissues: blood vessels marking neural tissue of the ONH shift temporally during 35° adduction in both young and older subjects, and nasally in abduction for younger individuals. In younger subjects, the temporal displacement in adduction was more than four-fold greater than the nasal shift in abduction. The greater magnitude of displacement in ad- in comparison with abduction is consistent with MRI findings that ON tethering occurs only in adduction[2,3,5]. However, one might have reasoned that if the ON sheath were to become tethered in adduction, resulting traction exerted on the globe-optic nerve junction would displace the ONH nasally relative to the retina. Instead, we observed a temporal shift in ONH vessels. This seemingly counter-intuitive finding likely resulted from "nasal buckling"[2] at the nasal edge of the globe-optic nerve junction, where in large adduction, an acute angle formed between the ON and sclera compresses the surrounding tissue to force the ONH anteriorly and temporally. The ON neural tissue shifts temporally relative to the sclera and ON sheath during ON tethering in adduction, as directly demonstrated by MRI.[27] Nasal buckling may also explain why in adduction the nasal half of the ONH and surrounding nasal PPR shift farther temporally than

the temporal half does. There may be less if any buckling in abduction, which may explain why only minor displacements are observed there in young adults, and none in older subjects. This again is consistent with MRI findings in abduction, where the slack ON generally remains centered within the ON sheath.

The ONH of young adults shifted more during both abduction and adduction than in older subjects. Young adults have more compliant ONH tissue than older individuals who accumulate structural changes and stiffening.[28,29] This age-related stiffening is even greater in African Americans and in people with glaucoma. Young adults generally have vitreous attached to the posterior retina, while elderly subjects often undergo vitreous liquefaction commonly resulting in PVD.[30] Nevertheless, individuals with complete PVD had ON and peripapillary deformation in adduction statistically similar to those with partial PVD. Literature suggests that aging is associated with tissue stiffening in the trabecular meshwork[31], lamina cribrosa[32–35], sclera[28,29,36,37], Bruch's membrane[38], and cornea[39]. The ONH can undergo extracellular matrix remodeling by altering the interplay between collagen and elastin fibers, changing the composition and concentration of matrix components, and by post-translational modifications (glycosylation, transglutamination, and crosslinking).[40] Additionally, older adults may have less orbital fat[41] that might allow the globe to retract more posteriorly into the orbit. This may increase ON sinuosity and decrease the path length that the ON must traverse during horizontal duction, and may attenuate ON tethering in adduction. Horizontal duction can generate strain at the ONH exceeding that caused by elevated IOP.[4,12] If adduction tethering does produce sufficient strain to cause optic neuropathy as predicted by biomechanical models,[12,18] then reduction of orbital fat to gain greater ON sinuosity might alleviate the strains during large adduction.

Differential shifts between adjacent zones in and around the ONH indicate that areas of the retina and ONH tissue are undergoing tensile or compressive shear in adduction. Among younger subjects, we observed an 18.3μm differential during adduction between the average horizontal shifts of the nasal and temporal halves of the ONH. This implies that the ONH is compressed while the nasal PPR is stretched. Compression of the ONH during adduction might impede capillary blood flow and damage the surrounding tissues. However, while the current study measured retinal blood vessel movements due to horizontal ductions, the study did not quantify blood flow. Future studies using techniques such as OCT angiography[42] could help elucidate whether large horizontal gaze duction hinder circulation in the ONH and retina.

Six of the current subjects exhibited pulsating ONH vessels due to the cardiac cycle. Previous literature has quantified the effect of vascular pulsatility in normal subjects and patients with glaucoma. The axial distance between the PPR and base of the normal optic disc cup (ADRC) reportedly fluctuates by 10.7±2.1μm and 11.6±1.8μm for the nasal and temporal sides of the ONH, respectively.[43] In patients with glaucoma, significantly higher ADRC fluctuations have been reported at 14.9±5.6μm and 14.0±4.9μm on nasal and temporal sides, respectively. Pulsatile displacements of approximately 10 μm may be innocuous to the ONH, so abduction-induced small nasal shifts are presumably undamaging. In adduction, however, the ONH is deformed four-fold as in abduction. Temporal deformations of the nasal half of the ONH in the current study were as high as 42μm,

averaging 36.5μm, well beyond the ADRC fluctuations observed in glaucoma. This observation supports the notion that repetitive strain from large adduction and adducting saccadic movements[44] occurring over a lifetime might cause gradual remodeling of the ONH leading to optic neuropathy in individuals who also have unfavorable combinations of scleral and optic nerve sheath biomechanical properties that concentrate the mechanical effects on vulnerable parts of the ON. Further investigation may determine whether horizontal gaze evoked ONH deformations are exaggerated in patients with glaucoma.

The present study was limited to detection of local vascular shifts relative to points of reference at the remote corners of the *en face* images that were assumed to be undeformed. All displacements reported here should be interpreted as local deformations of the ON and retina relative to the fixed reference points beyond 4 disc radii from its rim. Horizontal duction-induced translational changes to the whole posterior retina surface exceeding the imaging boundaries cannot be detected. Thus, if horizontal duction were to translate the entire globe, our method would not detect such changes. The current method is also insensitive to displacements in the anteroposterior direction that are observable by OCT. A previous OCT study identified 26° adduction as a threshold for marked gaze-evoked deformation of Bruch's membrane.[3] The current study did not include graded degrees of duction and thus cannot determine if any threshold exists for the observed displacements. Future studies could investigate whether such a threshold exists and may also explore effects of axial myopia and staphyloma on ONH deformations resulting from gaze shift. It could be predicted that duction-related ON and peripapillary deformations could be larger in high myopia, because globe axial elongation is associated with greater adduction tethering and prominent peripapillary atrophy and temporal ONH tilt.[45] Simple geometry suggests that an elongated globe necessitates a longer ON path length change during duction, and could amplify the effect of ON tethering to create greater ONH deformation during adduction. Future studies could also analyze tissue deformations in all 3 dimensions simultaneously from volumetric OCT angiography, although such an endeavor would be complicated by occlusions of multiple layers of vessels at the ONH.

In conclusion, 35° adduction displaces the nasal ha lf of the ON and adjacent PPR temporally. This displacement is greater in younger than older adults, and reflects deformation of the underlying retinal and neural tissue. Abduction causes a smaller but oppositely directed deformation observable only in young subjects. These shearing displacements in the ONH and adjacent PPR indicate tissue compression of the ONH.

Supplementary Material

Refer to Web version on PubMed Central for supplementary material.

ACKNOWLEDGEMENTS

a. Funding/Support: Supported by U.S. Public Health Service, National Eye Institute: Grants EY008313 and EY000331.

J. L. Demer is Arthur L. Rosenbaum Professor of Pediatric Ophthalmology.

b. Financial Disclosures: Joseph L. Demer: National Eye Institute Grant EY008313 and an Unrestricted Grant to the UCLA Department of Ophthalmology from Research to Prevent Blindness.

The following authors have no financial disclosures: Alan Le, Jessica Chen, Michael Lesgart, Bola A. Gawargious, and Soh Youn Suh.

c. Other Acknowledgements: none.

REFERENCES

1. Demer JL, Clark RA, Suh SY, et al. Magnetic resonance imaging of optic nerve traction during adduction in primary open-angle glaucoma with normal intraocular pressure. Invest Ophthalmol Vis Sci. 2017;58(10):4114–4125. [PubMed: 28829843]
2. Chang MY, Shin A, Park J, et al. Deformation of optic nerve head and peripapillary tissues by horizontal duction. Am J Ophthalmol. 2017;174:85–94. [PubMed: 27751810]
3. Suh SY, Le A, Shin A, Park J, Demer JL. Progressive deformation of the optic nerve head and peripapillary structures by graded horizontal duction. Invest Ophthalmol Vis Sci. 2017;58(12): 5015–5021. [PubMed: 28973373]
4. Wang X, Fisher LK, Milea D, Jonas JB, Girard MJ. Predictions of optic nerve traction forces and peripapillary tissue stresses following horizontal eye movements. Invest Ophthalmol Vis Sci. 2017;58(4):2044–2053. [PubMed: 28384725]
5. Suh SY, Clark RA, Demer JL. Optic nerve sheath tethering in adduction occurs in esotropia and hypertropia, but not in exotropia. Invest Ophthalmol Vis Sci. 2018;59(7):2899–2904. [PubMed: 30025141]
6. Anastasopoulos D, Ziavra N, Hollands M, Bronstein A. Gaze displacement and inter-segmental coordination during large whole body voluntary rotations. Exp Brain Res. 2009;193(3):323–336. [PubMed: 19002676]
7. Tomlinson RD, Bahra PS. Combined eye-head gaze shifts in the primate. I. Metrics. J Neurophysiol. 1986;56(6):1542–1557. [PubMed: 3806181]
8. Tomlinson RD, Bahra PS. Combined eye-head gaze shifts in the primate. II. Interactions between saccades and the vestibuloocular reflex. J Neurophysiol. 1986;56(6):1558–1570. [PubMed: 3806182]
9. Sibony PA. Gaze evoked deformations of the peripapillary retina in papilledema and ischemic optic neuropathy. Invest Ophthalmol Vis Sci. 2016;57(11):4979–4987. [PubMed: 27661851]
10. Burgoyne CF, Downs JC, Bellezza AJ, Suh JK, Hart RT. The optic nerve head as a biomechanical structure: a new paradigm for understanding the role of IOP-related stress and strain in the pathophysiology of glaucomatous optic nerve head damage. Prog. Retinal Eye Res. 2005;24(1): 39–73.
11. Burgoyne CF, Downs JC. Premise and prediction-how optic nerve head biomechanics underlies the susceptibility and clinical behavior of the aged optic nerve head. J Glaucoma. 2008;17(4):318–328. [PubMed: 18552618]
12. Wang X, Rumpel H, Lim WE, et al. Finite element analysis predicts large optic nerve head strains during horizontal eye movements. Invest Ophthalmol Vis Sci. 2016;57(6):2452–2462. [PubMed: 27149695]
13. Sigal IA, Ethier CR. Biomechanics of the optic nerve head. Exp Eye Res. 2009;88(4):799–807. [PubMed: 19217902]
14. Lee EJ, Kim TW, Weinreb RN. Reversal of lamina cribrosa displacement and thickness after trabeculectomy in glaucoma. Ophthalmology. 2012;119(7):1359–1366. [PubMed: 22464141]
15. Lee EJ, Kim TW, Weinreb RN, Kim H. Reversal of lamina cribrosa displacement after intraocular pressure reduction in open-angle glaucoma. Ophthalmology. 2013;120(3):553–559. [PubMed: 23218823]
16. Iwase A, Suzuki Y, Araie M, et al. The prevalence of primary open-angle glaucoma in Japanese: the Tajimi Study. Ophthalmology. 2004;111(9):1641–1648. [PubMed: 15350316]
17. Kim JH, Kang SY, Kim NR, et al. Prevalence and characteristics of glaucoma among Korean adults. Korean J Ophthalmol. 2011;25(2):110–115. [PubMed: 21461223]
18. Shin A, Yoo L, Park J, Demer JL. Finite element biomechanics of optic nerve sheath traction in adduction. J. Biomechanical Eng. 2017;139(10).

19. Jonas JB. Clinical implications of peripapillary atrophy in glaucoma. Curr Opin Ophthalmol. 2005;16(2):84–88. [PubMed: 15744137]
20. Wang X, Beotra MR, Tun TA, et al. In vivo 3-dimensional strain mapping confirms large optic nerve head deformations following horizontal eye movements. Invest Ophthalmol Vis Sci. 2016;57(13):5825–5833. [PubMed: 27802488]
21. Ruete C Ocular Physiology. 1999.
22. Leung CK, Chan WM, Hui YL, et al. Analysis of retinal nerve fiber layer and optic nerve head in glaucoma with different reference plane offsets, using optical coherence tomography. Invest Ophthalmol Vis Sci. 2005;46(3):891–899. [PubMed: 15728545]
23. Strouthidis NG, Fortune B, Yang H, Sigal IA, Burgoyne CF. Longitudinal change detected by spectral domain optical coherence tomography in the optic nerve head and peripapillary retina in experimental glaucoma. Invest Ophthalmol Vis Sci. 2011;52(3):1206–1219. [PubMed: 21217108]
24. Fortune B, Burgoyne CF, Cull GA, Reynaud J, Wang L. Structural and functional abnormalities of retinal ganglion cells measured in vivo at the onset of optic nerve head surface change in experimental glaucoma. Invest Ophthalmol Vis Sci. 2012;53(7):3939–3950. [PubMed: 22589428]
25. Fortune B, Reynaud J, Wang L, Burgoyne CF. Does optic nerve head surface topography change prior to loss of retinal nerve fiber layer thickness: a test of the site of injury hypothesis in experimental glaucoma. PLoS One. 2013;8(10):e77831. [PubMed: 24204989]
26. Medeiros FA, Alencar LM, Zangwill LM, Bowd C, Sample PA, Weinreb RN. Prediction of functional loss in glaucoma from progressive optic disc damage. Arch Ophthalmol. 2009;127(10): 1250–1256. [PubMed: 19822839]
27. Demer JL. Optic nerve sheath as a novel mechanical load on the globe in ocular duction. Invest Ophth Vis Sci. 2016;57(4):1826–1838.
28. Fazio MA, Grytz R, Morris JS, Bruno L, Girkin CA, Downs JC. Human scleral structural stiffness increases more rapidly with age in donors of African descent compared to donors of European descent. Invest Ophthalmol Vis Sci. 2014;55(11):7189–7198. [PubMed: 25237162]
29. Coudrillier B, Tian J, Alexander S, Myers KM, Quigley HA, Nguyen TD. Biomechanics of the human posterior sclera: age- and glaucoma-related changes measured using inflation testing. Invest Ophthalmol Vis Sci. 2012;53(4):1714–1728. [PubMed: 22395883]
30. Sebag J Structure, function, and age-related changes of the human vitreous. Bull Soc Belge Ophtalmol. 1987;223(Pt 1):37–57. [PubMed: 3307969]
31. Tektas OY, Lutjen-Drecoll E. Structural changes of the trabecular meshwork in different kinds of glaucoma. Exp Eye Res. 2009;88(4):769–775. [PubMed: 19114037]
32. Albon J, Karwatowski WS, Avery N, Easty DL, Duance VC. Changes in the collagenous matrix of the aging human lamina cribrosa. Br J Ophthalmol. 1995;79(4):368–375. [PubMed: 7742286]
33. Albon J, Karwatowski WS, Easty DL, Sims TJ, Duance VC. Age related changes in the non-collagenous components of the extracellular matrix of the human lamina cribrosa. Br J Ophthalmol. 2000;84(3):311–317. [PubMed: 10684844]
34. Albon J, Purslow PP, Karwatowski WS, Easty DL. Age related compliance of the lamina cribrosa in human eyes. Br J Ophthalmol. 2000;84(3):318–323. [PubMed: 10684845]
35. Leung LK, Ko MW, Lam DC. Effect of age-stiffening tissues and intraocular pressure on optic nerve damages. Mol Cell Biomech. 2012;9(2):157–173. [PubMed: 23113376]
36. Avetisov ES, Savitskaya NF, Vinetskaya MI, Iomdina EN. A study of biochemical and biomechanical qualities of normal and myopic eye sclera in humans of different age groups. Metab Pediatr Syst Ophthalmol. 1983;7(4):183–188. [PubMed: 6678372]
37. Geraghty B, Jones SW, Rama P, Akhtar R, Elsheikh A. Age-related variations in the biomechanical properties of human sclera. J Mech Behav Biomed Mater. 2012;16:181–191. [PubMed: 23182387]
38. Booij JC, Baas DC, Beisekeeva J, Gorgels TG, Bergen AA. The dynamic nature of Bruch's membrane. Progress in retinal and eye research. 2010;29(1):1–18. [PubMed: 19747980]
39. Malik NS, Moss SJ, Ahmed N, Furth AJ, Wall RS, Meek KM. Ageing of the human corneal stroma: structural and biochemical changes. Biochim Biophys Acta. 1992;1138(3):222–228. [PubMed: 1547284]
40. Liu B, McNally S, Kilpatrick JI, Jarvis SP, O'Brien CJ. Aging and ocular tissue stiffness in glaucoma. Surv Ophthalmol. 2018;63(1):56–74. [PubMed: 28666629]

41. Salvi SM, Akhtar S, Currie Z. Ageing changes in the eye. Postgrad Med J. 2006;82(971):581–587. [PubMed: 16954455]

42. Mansoori T, Sivaswamy J, Gamalapati JS, Agraharam SG, Balakrishna N. Measurement of radial peripapillary capillary density in the normal human retina using optical coherence tomography angiography. J Glaucoma. 2017;26(3):241–246. [PubMed: 27906811]

43. Singh K, Dion C, Godin AG, et al. Pulsatile movement of the optic nerve head and the peripapillary retina in normal subjects and in glaucoma. Invest Ophthalmol Vis Sci. 2012;53(12): 7819–7824. [PubMed: 23099495]

44. Wu CC, Kowler E. Timing of saccadic eye movements during visual search for multiple targets. J Vis. 2013;13(11).

45. Kim TW, Kim M, Weinreb RN, Woo SJ, Park KH, Hwang JM. Optic disc change with incipient myopia of childhood. Ophthalmology. 2012;119(1):21–26 e21–23. [PubMed: 21978594]

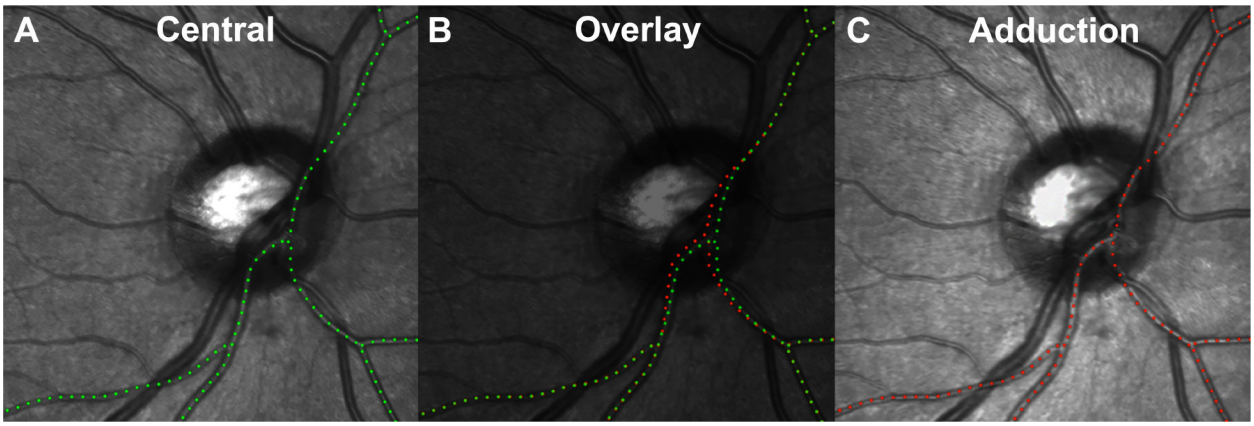

Fig. 1.

Images obtained in central gaze (A) and 35° adduct ion (C) in which a large blood vessel has been marked with green and red dots, respectively. Vessel displacements due to gaze change indicate deformation of the underlying retina, and were determined by image superimposition (B). Temporal shifting of vessel on the ONH is evident.

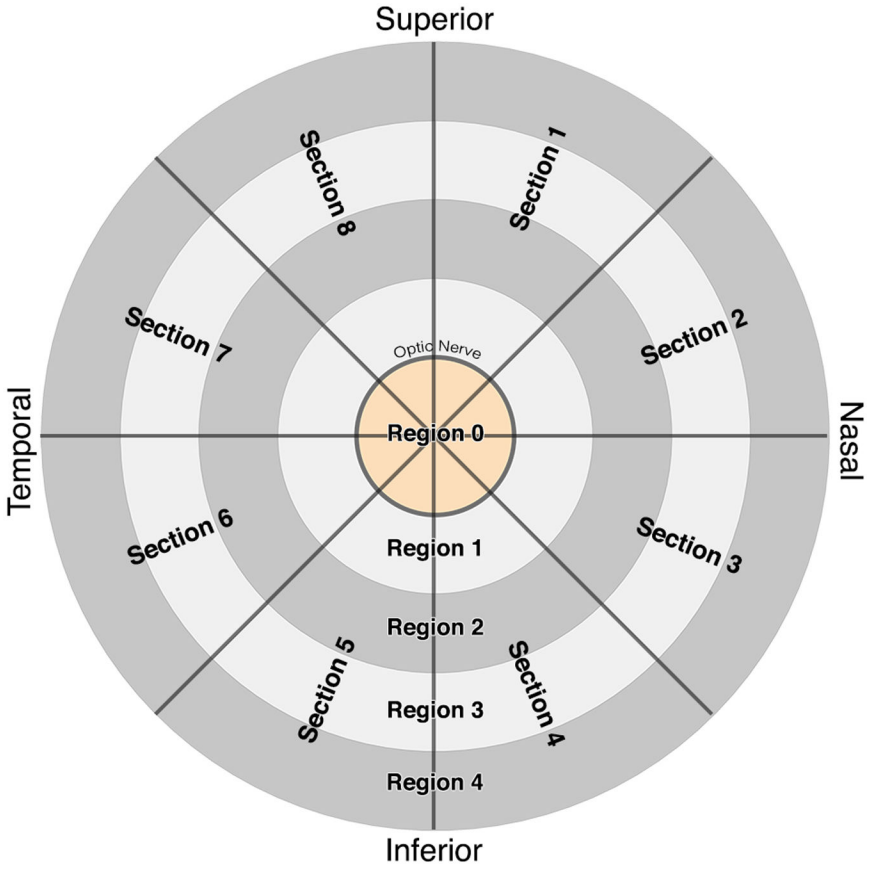

Fig. 2.

For analysis, images were divided into 40 different zones using a circular grid. Region 0 represented the ONH itself. Each concentric region was a multiple of ONH diameter, and divided into 8 sections at 45° each. Sections 1–4 and Sections 5–8 represented the nasal and temporal halves of the ONH, respectively.

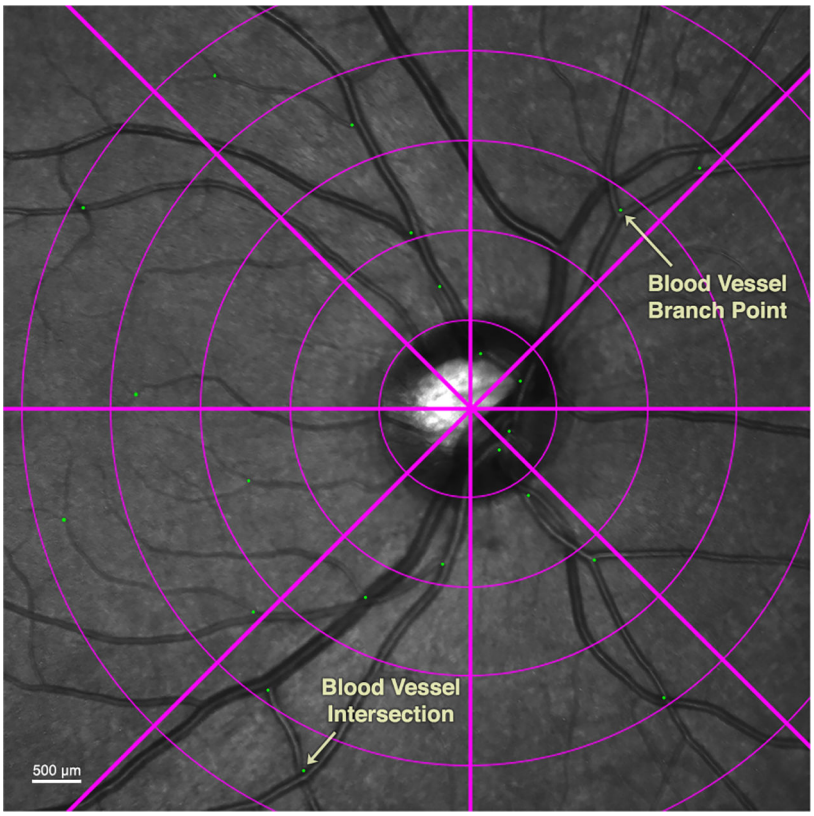

Fig. 3.
Green dot fiducials were placed at vascular branches and intersections.

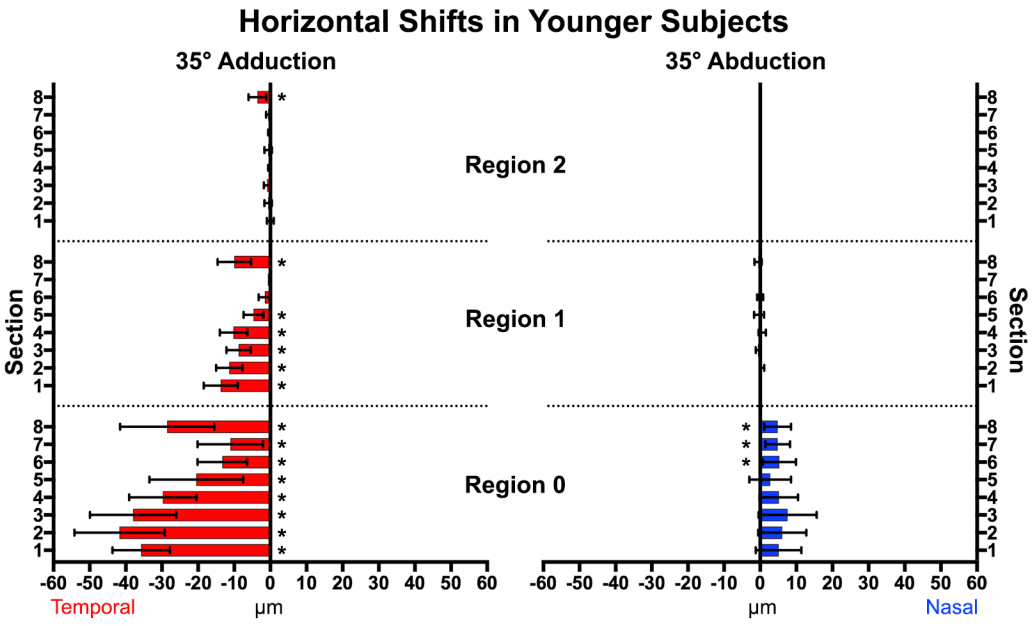

Fig. 4.

Vessel displacement during 35° horizontal duction of younger subjects. All sections within the optic nerve head (Region 0) and the majority of Region 1 showed significant temporal shifts in adduction (left), with fewer and smaller shifts nasally in abduction. * represents significant non-zero displacements. Brackets mark 95% confidence intervals.

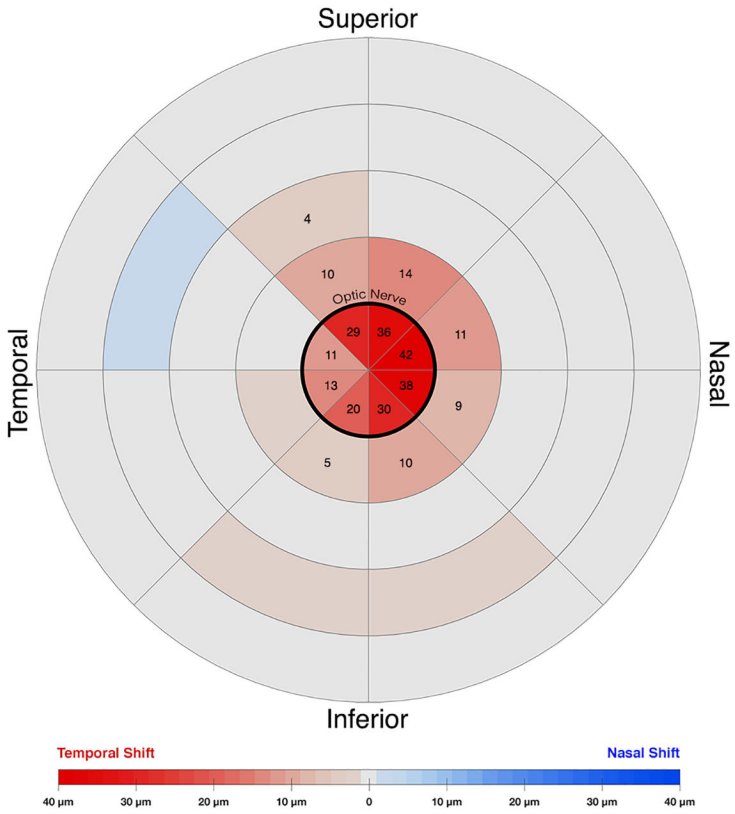

Fig. 5.

Horizontal displacement heatmap during adduction in younger subjects. The center circle represents the optic nerve head. Temporal shifts are colored red, nasal shifts blue. Numbers denote zones exhibiting significant displacement during adduction. The nasal half of the nerve head showed the greatest temporal deformation.

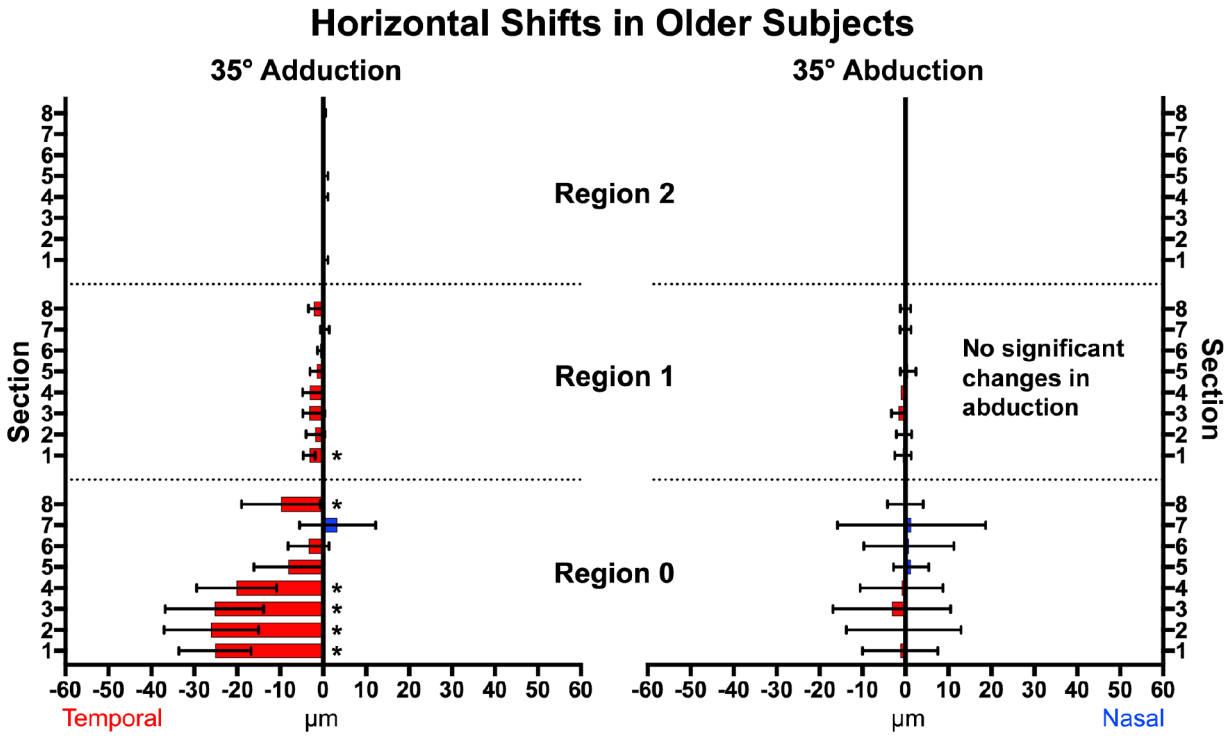

Fig. 6.

Horizontal displacement in older subjects during adduction (left) and abduction (right). In adduction, the nasal half (Sections 1–4) of the optic nerve head (Region 0) exhibited greatest temporal shift while there were smaller temporal displacements in Region 1. There were no significant displacements in abduction. * signifies non-zero displacements. Brackets mark 95% confidence intervals.

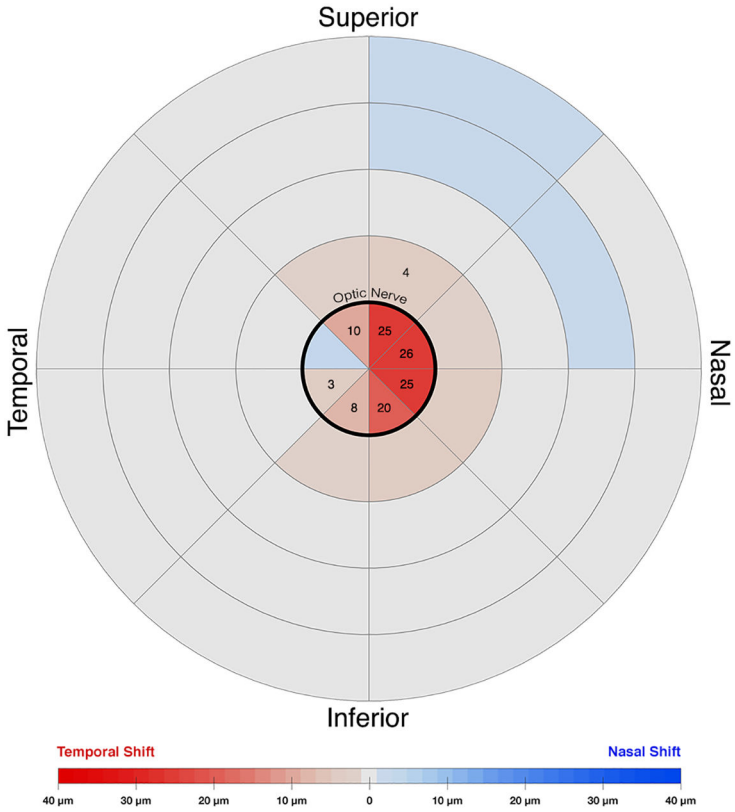

Fig. 7.

Horizontal displacement heatmap for adduction in older subjects. The center circle represents the optic nerve head. Temporal shifts are colored red. Nasal shifts are colored blue. Numbers on the map denote zones that had a significant change during adduction. The nasal half of the nerve head exhibited more temporal deformation. There was less overall deformation than in younger subjects.

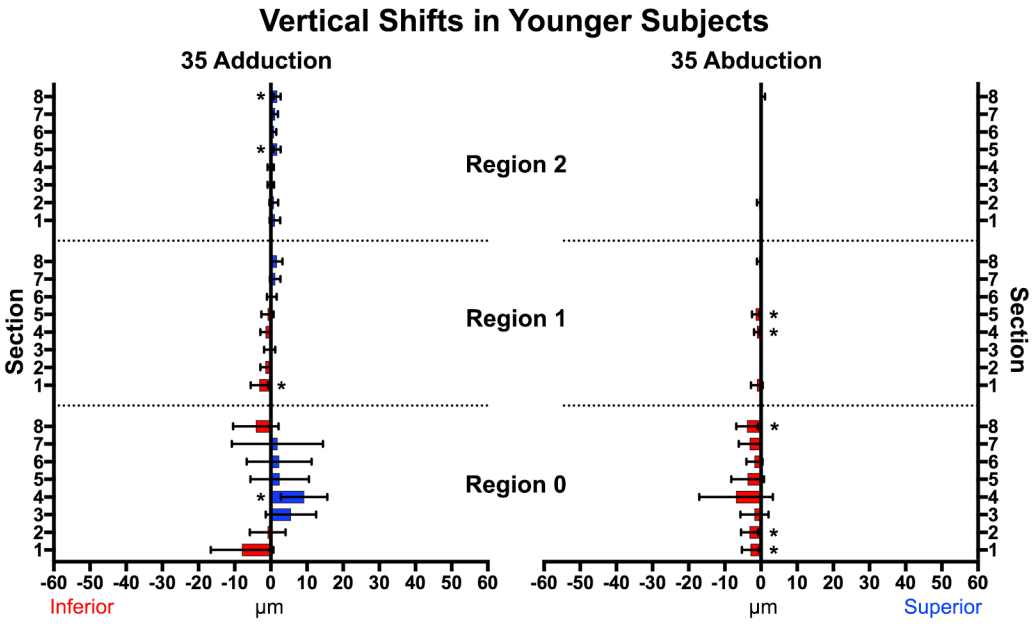

Fig. 8.

In younger subjects, neither adduction not abduction caused major vertical displacements of the optic nerve head or papillary retina. * represents statistically significant (P<0.02) but mechanically trivial displacements. Brackets mark 95% confidence intervals.

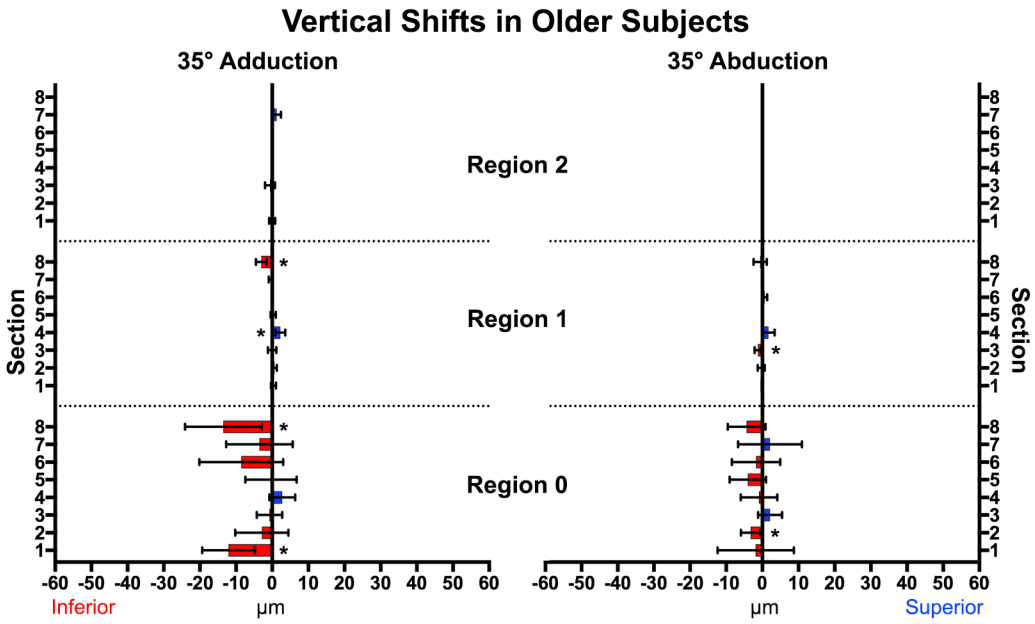

Fig. 9.

In older subjects, the superior half of the ONH shifted inferiorly in adduction. * represents significant (P<0.02) non-zero displacements. Brackets mark 95% confidence intervals.